

# Magnetic Properties of FeCoWYB-based Ferromagnetic Alloys with a Small Addition of Pt

PAWEL PIETRUSIEWICZ\*

Institute of Physics, Czestochowa University of Technology, Armii Krajowej 19 Av., 42-200 Czestochowa, Poland

The paper presents the results of research on the effect of Pt addition in the amount of 2 to 3% at. in to bulk  $Fe_{61}Co_{10}B_{20}Y_{8-x}W_1Pt_x$  alloy on its structure and magnetic properties. Alloys in the form of tiles were made by pressing a liquid alloy into a copper liquid-cooled mold. Structural examinations were carried out using X-ray diffraction (XRD). The magnetic properties were examined using a vibration magnetometer (VSM). Based on structural investigations, the occurrence of crystalline phases, i.e.:  $\alpha$ -Fe, Fe<sub>3</sub>B, FePt, Fe<sub>3</sub>Pt, FePt<sub>7</sub>, was found. The results of VSM tests showed that both saturation magnetization ( $m_0M_s$ ) and coercive field ( $H_c$ ) significantly increased. The study showed that even a small change in the Pt content in the alloy affects its structure and thus significantly affects the magnetic properties.

Keywords: bulk alloys, saturation moments, spin waves, x-ray, crystalline structure

Extensive research on amorphous and nanocrystalline alloys based on Fe has been carried out over the last several decades. One of the newer groups of Fe-based materials are the so-called massive amorphous and nanocrystalline alloys. Depending on the chemical composition, these alloys have interesting magnetic and mechanical properties [1]. However, it should be distinguished because of their thickness on classic materials and massive amorphous materials. Classical amorphous tape materials show slightly different parameter values than massive amorphous alloys, with same composition. In this case, special attention should be paid to alloys based on transition metals (metal - metalloid) from the Fe Co and B [2] groups. Massive amorphous alloys are obtained based on universally accepted criteria developed by A. Inoue [3].

Generally, all papers in which alloys with Pt content are examined, are concerned to be hard magnetic materials [4-6]. In these works it was found that the improvement of magnetically hard properties is obtained after the addition of at least 5% at. Pt. The precursor for obtaining magnetically hard materials are rapid-cooled tapes, usually with an amorphous structure [7-12]. As a result of heat treatment of the amorphous tapes, single-phase or polinary phase alloys rich in different crystalline phases based on Fe, Pt and other metals can be obtained [13-24].

In FeCoB alloys with the addition of Pt, ordered and unordered phases can be created with face-centered-cubic symmetries (fcc = A1 and L1<sub>2</sub>) and ordered phases with face-centered-tetragonal symmetry (fct = L1<sub>0</sub>) with high uniaxial magnetocrystalline anisotropy (7 MJ/m<sup>3</sup>) [7].

The paper presents the results of investigations on the influence of a small Pt additive on the structure and magnetic properties of ferromagnetic alloy  $Fe_{61}Co_{10}B_{20}Y_{8-x}W_1Pt_x$  (where x = 2, 3) in the form of plates in the solidified state.

## Experimental part

Samples with composition  $Fe_{61}Co_{10}B_{20}Y_{8-x}W_1Pt_x$  (where x = 2, 3) were made of high purity components: Fe - 99.95% at., Co - 99.95% at., B - 99.5% at., Y - 99, 95% at. W - 99.95% at., Pt - 99.95%, at. Alloy ingots were melted several times in an arc furnace in order to homogenize their structure. The process was carried out in a protective atmosphere of argon. The material samples in the form of

plates with a thickness of 0.5 mm were made by pressing a liquid alloy into a copper liquid-cooled form. The research on the structure of the samples in the state after solidification and low energy powdering was carried out using an X-ray diffractometer (XRD) Bruker D-8 Advance. The XRD measurement was made in the angle of 2 $\theta$  from 30° to 100° with a measuring step of 0.02° and exposure time of 10s per step. Measurements of magnetic properties were made using a vibration magnetometer (VSM) from LakeShore, working in a magnetic field with an induction up to 2T). On the basis of VSM measurements saturation magnetization ( $\mu_0M_s$ ) and coercive field ( $H_c$ ) were determined. Analysis of the primary magnetization curves in the high magnetic fields, the spin wave stiffness parameter ( $D_{sp}$ ) was determined.

## Results and discussions

In figure 1, the X-ray diffraction patterns measured for the alloy samples in the form of plates with 0.5 mm thickness are shown  $Fe_{61}Co_{10}B_{20}Y_{8-x}W_1Pt_x$  (where x = 2, 3).

The X-ray diffraction pattern of the  $Fe_{61}Co_{10}B_{20}Y_7W_1Pt_2$  alloy shown in figure 1 is typical of two-phase alloy consisting of an amorphous and a crystalline part. On the diffractogram, in the range of 2 $\theta$  angle from 35 to 55°, an broad amorphous maximum, on which there are numerous

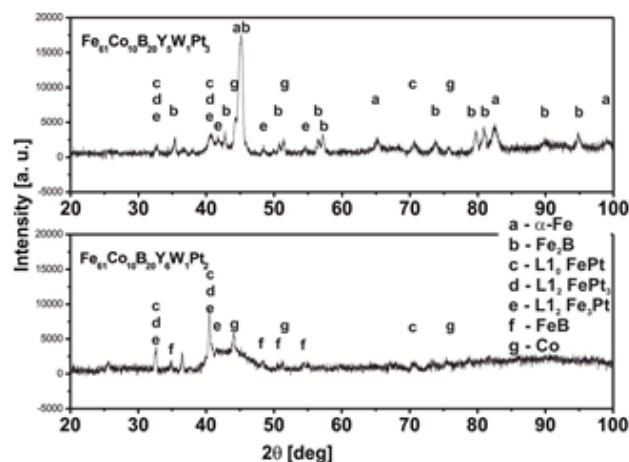


Fig. 1. X-ray diffraction patterns for the plate-form samples of the investigated alloys

\* email: pietrusiewicz.pawel@wip.pcz.pl

broad peaks of low intensity, is visible. The width and intensity of these peaks is characteristic of the poorly developed crystalline structures described by the small grain size. In the case of the second alloy, a significant part of the amorphous matrix was rebuilt into various types of crystalline phases: a-Fe, Fe<sub>2</sub>B, FeB, L1<sub>0</sub>-FePt, L1<sub>2</sub>-FePt<sub>3</sub>, L1<sub>2</sub>-Fe<sub>3</sub>Pt, Co. Phases a-Fe, Fe<sub>2</sub>B, FeB and Co are commonly known and do not require detailed description [1, 2]. On the other hand, crystalline phases of Fe-Pt are much more interesting. The phases designated as L1<sub>0</sub> and L1<sub>2</sub>-Fe<sub>3</sub>Pt, characterized with the elemental cell with tetragonal and cubic order respectively are described in the literature as phases with ferromagnetic ordering [8]. The crystalline phase L1<sub>2</sub>-FePt<sub>3</sub> with a cubic elementary cell (fcc) has paramagnetic properties [9]. The change in the proportion of crystalline phases in the volume of the alloy depending on the Pt content at the cost of Y influences the magnetic properties of the samples. In figure 2 static magnetic hysteresis loops measured for Fe<sub>61</sub>Co<sub>10</sub>B<sub>20</sub>Y<sub>8-x</sub>W<sub>1</sub>Pt<sub>x</sub> alloys (where x = 2, 3) in the solidified state are shown. For the alloy sample Fe<sub>61</sub>Co<sub>10</sub>B<sub>20</sub>Y<sub>7</sub>W<sub>1</sub>Pt<sub>2</sub>, the static hysteresis loop has a typical shape as for magnetic materials exhibiting magnetically soft properties. Due to the very nature of the alloy structure, in which the amorphous structure is definitely larger, one can observe an almost rectangular magnetization shape of this material.

FeCoB-based amorphous alloys are characterized by magnetostriction close to zero, low restraining intensity and, therefore, almost rectangular Ewing's knee. Although in the Fe<sub>61</sub>Co<sub>10</sub>B<sub>20</sub>Y<sub>7</sub>W<sub>1</sub>Pt<sub>2</sub> alloy the presence of magnetically hard phases is primarily observed and the residual content of pure Co, this alloy achieves magnetization saturation at a lower magnetic field than the second investigated alloy. The fact of the appearance of three soft magnetic phases in the Fe<sub>61</sub>Co<sub>10</sub>B<sub>20</sub>Y<sub>5</sub>W<sub>1</sub>Pt<sub>3</sub> alloy in relation to the Fe<sub>61</sub>Co<sub>10</sub>B<sub>20</sub>Y<sub>7</sub>W<sub>1</sub>Pt<sub>2</sub> alloy (where there are no phases) is not a reason to improve the soft magnetic properties and in particular reduce the coercive field ( $H_c$ ), as would be expected (table 1, fig. 2).

The presence of these soft magnetic phases strongly influenced the value of saturation, which increased by nearly 0.3 T. Unfortunately, the large variation of the magnetic structure in this sample has a negative effect on the process of magnetization near the area called the approach to ferromagnetic saturation. This is manifested

by a significant defect of the magnetic structure and a shift towards higher magnetic fields, and thus the impact of structural defects on the high-field magnetization process. This phenomenon is depicted in figure 3.

On the basis of static magnetic hysteresis loops analysis, magnetic parameters such as saturation magnetization ( $\mu_0 M_s$ ) and coercive field ( $H_c$ ) were determined (table 1).

In high magnetic fields, when the defects of the structure are no longer affected by the magnetizing process, their role is taken over by spin waves, which slow it down as a result of thermal vibrations [9]. A linear relationship is then observed  $\mu_0 M_s ((\mu_0 H)^{1/2})$  (fig. 3.) related to the Holstein - Primakoff [10] process. This change in the value of the magnetic field starting this process is up to twice as high for the alloy Fe<sub>61</sub>Co<sub>10</sub>B<sub>20</sub>Y<sub>5</sub>W<sub>1</sub>Pt<sub>3</sub> (1.14 T) than for Fe<sub>61</sub>Co<sub>10</sub>B<sub>20</sub>Y<sub>7</sub>W<sub>1</sub>Pt<sub>2</sub> (0.52 T) alloy.

Based on the numerical analysis with the formula (1), the parameter ( $D_{sp}$ ) was determined describing the spin wave stiffness [11]:

$$b = 3,54 g \mu_B \mu_s \left( \frac{1}{4\pi D_{sp}} \right)^{1/2} kT (g \mu_B)^{1/2} \quad (1)$$

where:  $b$  - the slope of the linear fit line  $\mu_0 M_s ((\mu_0 H)^{1/2})$ ,  $k$  - Boltzman constant,  $\mu_B$  - Bohrs magneton,  $g$  - gyromagnetic factor.

The  $D_{sp}$  parameter is very sensitive to changes in the indirect  $sp$  environment of magnetic atoms. Its growth is related to the greater number of directly adjacent magnetic atoms, in our case it is mainly about the magnetic interactions between the three possible configurations of the Fe-Fe, Fe-Co and Co-Co atoms. In the case of the investigated alloys, as indicated by the results (table 1), the  $D_{sp}$  parameter should have a higher value for the Fe<sub>61</sub>Co<sub>10</sub>B<sub>20</sub>Y<sub>5</sub>W<sub>1</sub>Pt<sub>3</sub> alloy and yet this is not the case. Most likely, the change in the amorphous matrix contribution in the melt volume has a direct effect on the  $D_{sp}$  value. It should be assumed that in the case of the Fe<sub>61</sub>Co<sub>10</sub>B<sub>20</sub>Y<sub>7</sub>W<sub>1</sub>Pt<sub>2</sub> alloy, the amorphous matrix fraction is over 90%, which is why an almost rectangular shape of the static hysteresis loop is observed. It can be concluded that the magnetic structure is more homogeneous, which confirms the value of the  $D_{sp}$  parameter. For the Fe<sub>61</sub>Co<sub>10</sub>B<sub>20</sub>Y<sub>5</sub>W<sub>1</sub>Pt<sub>3</sub> alloy sample, despite the appearance of several soft magnetic phases, the magnetization process itself (fig. 3) and the calculated value of the  $D_{sp}$  parameter

**Table 1**

DATA FROM ANALYSIS OF THE STATIC HYSTERESIS LOOPS (VSM) FOR Fe<sub>61</sub>Co<sub>10</sub>B<sub>20</sub>Y<sub>8-x</sub>W<sub>1</sub>Pt<sub>x</sub>, WHERE:

$\mu_0 M_s$  - SATURATION MAGNETIZATION,  $H_c$  - COERCIVITY,  $D_{sp}$  - SPIN WAVE STIFFNESS PARAMETER

	$\mu_0 M_s$ [ T ]	$H_c$ [ A/m ]	$D_{sp}$ [ $10^{-2} \text{ meV nm}^2$ ]	Ref
Fe <sub>61</sub> Co <sub>10</sub> B <sub>20</sub> Y <sub>6</sub> W <sub>1</sub> Pt <sub>2</sub>	1.20(2)	934	43	[12]
Fe <sub>61</sub> Co <sub>10</sub> B <sub>20</sub> Y <sub>5</sub> W <sub>1</sub> Pt <sub>3</sub>	1.47(2)	12736	36	

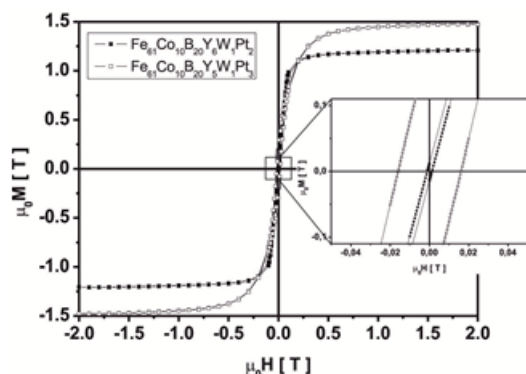


Fig. 2. Static hysteresis loops for the investigated samples

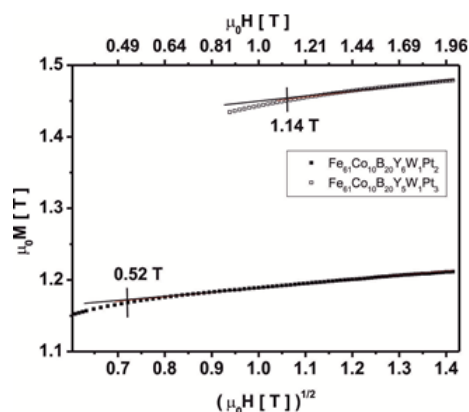


Fig. 3. Magnetic saturation ( $\mu_0 M_s$ ) of the alloy in the as-cast state as a function of  $(\mu_0 H)^{1/2}$

indicate a large defect in the magnetic structure. The value of the  $D_{sp}$  parameter is smaller because there are many different configurations between magnetic atoms associated with the occurrence of different magnetic phases. Higher magnetization value for the alloy  $Fe_{61}Co_{10}B_{20}Y_5W_1Pt_3$  may be also related to decrease of Y content, whose atomic radius is 180 pm. In the case when the atom Y finds itself between the magnetic atoms Fe or Co, the correlation between ferromagnetic interactions decreases.

## Conclusions

Change in Pt and Y content in rapid-cooled FeCoB alloys influences the change of the amorphous matrix proportion with respect to crystalline phases. In the  $Fe_{61}Co_{10}B_{20}Y_5W_1Pt_3$  alloy, an increase in the Pt content at the expense of Y is the reason for the formation of new crystalline systems without the participation of Pt, which additionally affects the blocking formation of the crystalline FeB phase. For the alloy sample  $Fe_{61}Co_{10}B_{20}Y_6W_1Pt_2$ , a significantly higher value of the  $D_{sp}$  parameter was obtained than for the second alloy. This means that in the case of designing ferromagnetic two-phase alloys, the contribution of the amorphous matrix to the volume of the alloy in relation to the crystalline phases should be taken into account.

## References

1. MCHENRY, M. E., WILLARD, M. A., LAUGHLIN, D. E., Prog. Mater. Sci. **44**, 1999, p. 291
2. GRABIAS, A., KOPCEWICZ, M., LATUCH, J., OLESZAK, D., PĚKAŁA, M., KOWALCZYK, M., J. Magn. Magn. Mater. **434**, 2017, p. 126
3. INOUE, A., Acta Mater. **48**, 2000, p. 279
4. ZHANG, W., MA, D., LI, Y., YUBUTA, K., LIANG, X., PENG, D., J. Alloy Compd. **615**, 2014, p. S252
5. RANDRIANANTOANDRO, N., CRISAN, A. D., CRISAN, O., MARCIN, J., KOVAC, J., HANKO, J., GRENĚCHE, J. M., SVEC, P., CHROBAK, A., SKORVANEK, I., J. Appl. Phys. **108**, 2010, p. 093910
6. HWANG, S-W., KIM, S.J., YOON, C.S., KIM, C.K., Phys. Stat. Sol. A **201**, 2004, p. 1875

7. CRISAN, A.D., CRISAN, O., RANDRIANANTOANDRO, N., VALEANU, M., MORARIU, M., BURKEL, E., Mater. Sci. Eng. C **27**, 2007, p. 1283
8. MENSHIKOV, A., TARNOCZI, T., KREN, E., Phys. Stat. Sol. A **28**, 1975, p. K85
9. HOLSTEIN, T., PRIMAKOFF, H., Phys. Rev., **59**, 1941, p. 388.
10. BLOCH, K., Rev. Chim.(Bucharest) **68**, no. 3, 2017, p. 478
11. PIETRUSIEWICZ, P., Acta Phys. Pol. A **133**, 2018, p. 666
12. NABIALEK, M., JEZ, B., JEZ, K., Rev. Chim.(Bucharest), **69**, no. 9, 2018, p. 2546.
13. TANASE, S.I., TANASE, D., DOBROMIR, M., SANDU, A.V., GEORGESCU, V., Journal of Superconductivity and Novel Magnetism, **29**, no. 2, 2016, p. 469.
14. TANASE, S.I., TANASE, D., SANDU, A.V., GEORGESCU, V., Journal of Superconductivity and Novel Magnetism, **25**, no. 6, 2012, p. 2053.
15. NABIALEK, M., BLOCH, K., SZOTA, M., SANDU, A.V., Mat. Plast., **54**, no. 3, 2017, p. 491.
16. VLAD, L., SANDU, A.V., GEORGESCU, V., Journal of Superconductivity and Novel Magnetism, **25**, no. 2, 2012, p. 469.
17. POIANA, M., DOBROMIR, M., NICA, V., SANDU, I., GEORGESCU, V., Journal of Superconductivity and Novel Magnetism, **26**, no. 10, 2013, p. 3105. DOI: 10.1007/s10948-013-2126-3.
18. SULITANU, N., SANDU, I., Rev. Chim.(Bucharest), **54**, no. 7, 2003, p. 561.
19. SULITANU, N., PIRGHIE, C., SANDU, I., Rev. Chim.(Bucharest), **58**, no. 1, 2007, p. 20.
20. VIZUREANU, P., Environmental Engineering And Management Journal, **8**, no. 2, 2009, p. 301
21. PLATON, M.A., STEF, M., POPA, C., TIUC, A.E., NEMES, O., IOP Conference Series-Materials Science and Engineering, **374**, 2018, UNSP 012065.
22. TIUC, A.E., NEMES, O., PERHAITA, I., VERMESAN, H., GABOR, T., DAN, V., Studia Universitatis Babes-Bolyai Chemia, **60**, no. 2, 2015, p. 169.
23. ACHITEI, D., GALUSCA, D.G., VIZUREANU, P., CARABET, R., CIMPOESU, N., Metalurgia International, **14**, 2009, p. 45
24. VIZUREANU, P., PERJU, M.C., GALUSCA, D.G., NEJNERU, C., AGOP, M., Metalurgia International, vol. XV, no. 12, 2010, p. 59-64.

Manuscript received: 14.08.2018